

Off-design performance of supercritical compressed carbon dioxide energy storage system

Mingzhi Zhao^{1,2}, Yilin Zhu^{1,2}, Dongzi Hu^{1,3}, Yujie Xu^{1,2*}, Haisheng Chen^{1,2*}

1 Institute of Engineering Thermophysics, Chinese Academy of Sciences, Beijing 100190, China

2 University of Chinese Academy of Sciences, Beijing 100049, China

3 North China Electric Power University, Beijing 102206, China

(*Corresponding Author: chen_hs@mail.etp.ac.cn)

ABSTRACT

Energy storage is a supporting technology to achieve large-scale consumption of renewable energy and smart grid. Supercritical compressed carbon dioxide energy storage (SC-CCES) system is an appealing physical energy storage thanks to its compact system structure and high round-trip efficiency. However, in previous studies, the temperature and pressure of storage chamber are traditionally set to a constant value, there is a lack of thermodynamic analysis for SC-CCES system from the perspective of storage chambers interactively varying, which results in compressor and turbine operating consistently at off-design conditions. Hence, the off-design performance of SC-CCES system is investigated. The parametric analysis is conducted to evaluate the influence of system parameters and the optimization design platform is established to explore the optimization potential. Results indicate that round-trip efficiency and energy density of SC-CCES system present opposite varying trends with increasing compressor efficiency and the initial temperature of charge in low-pressure storage chamber. The optimal round-trip efficiency of SC-CCES system is achieved as 78.14 %, along with the optimal energy density of 0.2580 kWh/m³.

Keywords: supercritical compressed carbon dioxide energy storage, off-design, storage chamber, thermodynamic analysis, system optimization

NONMENCLATURE

Abbreviations

AMGA	Archive-based micro genetic algorithm
CCES	Compressed CO ₂ energy storage
HSC	High-pressure sCO ₂ storage chamber
HWT	Hot water tank
HE	Heat exchanger
LCES	Liquid CO ₂ energy storage
LSC	Low-pressure sCO ₂ storage chamber
LWT	Cold water tank
sCO ₂	Supercritical CO ₂
SC-CCES	Supercritical compressed CO ₂ energy storage
TC-CCES	Transcritical compressed CO ₂ energy storage
<i>Symbols</i>	
n	Year
E	Energy density
h	Enthalpy
\dot{m}	Mass flow
M	Mass
\dot{n}	Rotation speed
P	Pressure
t	Time
T	Temperature
W	Power
ε	Compression ratio
π	Expansion ratio
η	Efficiency
<i>Subscript</i>	
0	Design value
c	Compressor
in	Inlet
init	Initial

out	Outlet
s	Iisentropic
t	Turbine
term	Terminal

1. INTRODUCTION

Due to the requirements of a low-carbon economy, the utilization of renewable energy is experiencing rapid growth. However, renewable energy sources such as wind and solar are intermittent and unstable, requiring integration with energy storage systems to ensure the provision of high-quality electrical power supply [1,2].

An increasingly attention has been devoted to compressed carbon dioxide energy storage (CCES) system in recent years [3-14]. Among them, Sun et al. [3] proposed a liquid CO₂ energy storage (LCES) system with low-pressure stores, which stores cold energy using methanol and latent cold storage to liquefy discharged CO₂ after expansion. The analysis results indicate that the round-trip efficiency and energy density of the system can be 51.45 % and 22.21 kWh/m³ respectively. Chae et al. [4] conducted a thermodynamic analysis of an integrated LCES system with steam cycle of thermal power plant, which achieves a round-trip efficiency of 46 % and an energy density of 36 kWh/m³. Despite LCES system owning a higher energy storage density, the necessity for liquefaction storage on both the high-pressure and low-pressure processes leads to system complexity as well as a comparatively lower round-trip efficiency [5,6].

It is worthwhile to note that transcritical compressed CO₂ energy storage (TC-CCES) system and supercritical compressed CO₂ energy storage (SC-CCES) system are emerging and developing rapidly, aiming to achieve superior round-trip efficiency [7,8]. As for steady-thermodynamic analysis, Liu et al. [9] compared a two-reservoir CCES system using saline-aquifer reservoirs to store CO₂ under supercritical and transcritical conditions. They found that the configuration of SC-CCES system is simpler with the round-trip efficiency reaching 62.28 %. Wu et al. [10] developed a conventional TC-CCES system with liquid CO₂ stored in a low-pressure storage tank, and it indicates that the cold energy storage unit of liquid CO₂ has the highest exergy destructions. Additionally, the performance and stability of the compressor are significantly affected by the abrupt change of CO₂ properties approaching the critical point [11,12]. Specifically, it is difficult to achieve transcritical carbon dioxide compression concerning impeller-type

compressors, for which TC-CCES system cannot be applied in large-scale energy storage [13]. Furthermore, He et al. [14] revealed the sources of energy-saving potential of each component of SC-CCES system through advanced exergy analysis, achieving an exergy efficiency of 57.02 %.

It highlights that the previous research on SC-CCES system has predominantly concentrated on steady-state conditions. However, during the charging process, the pressure and temperature of the low-pressure storage chamber decrease continuously, the pressure and temperature of the high-pressure storage chamber increase continuously, and the compression ratio of the compressor increases continuously. During the discharging process, the pressure and temperature of the high-pressure storage chamber are constantly reduced, the pressure and temperature of the low-pressure storage chamber are constantly increased, and the expansion ratio of the turbine is constantly reduced. This makes SC-CCES system always operate under off-design conditions. Consequently, it is necessary to study thermodynamic performance of SC-CCES system under off-design conditions.

In this paper, the off-design performance of SC-CCES system is investigated. Furthermore, the effects of some key parameters on system performance are studied through parametric analysis. Finally, the bi-objective optimization of round-trip efficiency and energy density is carried out by using archive-based micro genetic algorithm (AMGA). This study has important theoretical and application value.

2. SYSTEM DESCRIPTION

The schematic of SC-CCES system is illustrated in Fig. 1, consisting of a high-pressure supercritical carbon dioxide (sCO₂) storage chamber (HSC), a low-pressure sCO₂ storage chamber (LSC), a compressor unit, a turbine unit, two heat exchangers (HE), cold water tank (LWT), and hot water tank (HWT). During the charging process, the sCO₂ coming from LSC is compressed to the same pressure as HSC after flowing through the compressor and then cooled to the same temperature as HSC by water from LWT, until the pressure of HSC increases to the setting value and the pressure of LSC decreases to the setting value. During the discharging process, the sCO₂ originating from the HSC is heated by water from HWT and then expand to the same pressure as LSC, until the pressure of HSC equals the pressure of LSC.

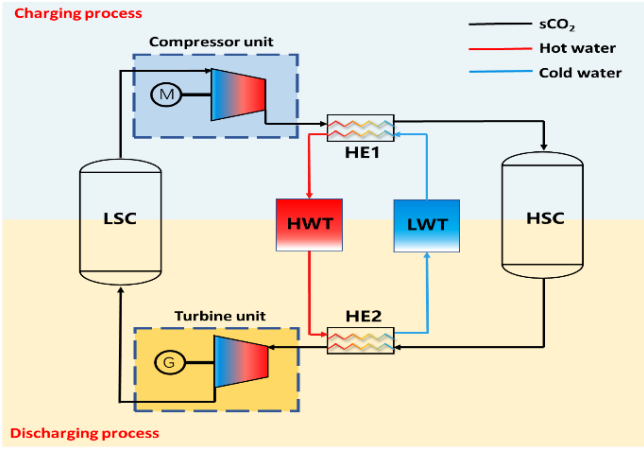


Fig. 1. Schematic of SC-CCES system

3. METHODOLOGY

In this paper, the thermodynamic properties of working fluids are calculated by using MATLAB software and REFPROP 9.1 software. As for the SC-CCES system, the following assumptions are presented herein:

- (1) Pressure losses in heat exchangers, energy storage devices, and pipelines are neglected.
- (2) Heat losses of components and pipelines are not taken into account.
- (3) The minimum pinch temperature difference for heat exchangers is set to 5 °C.

3.1 Mathematical model

3.1.1 Compressor

The isentropic efficiency and power of the compressor are shown as equations (1)-(2):

$$\eta_c = (h_{out,c,s} - h_{in,c}) / (h_{out,c} - h_{in,c}) \quad (1)$$

$$W_c = \dot{m}_c (h_{out,c} - h_{in,c}) \quad (2)$$

The influence of off-design state on the isentropic efficiency η_c during compression is considered. ε is the compression ratio ($\varepsilon = P_{c,out} / P_{c,in}$). Off-design performance model of the compressor is established by using characteristic maps [15,16], which is calculated as

$$\varepsilon / \varepsilon_0 = c_1 (\dot{n}_c) \dot{G}_c^2 + c_2 (\dot{n}_c) \dot{G}_c + c_3 (\dot{n}_c) \quad (3)$$

$$\eta_c / \eta_{c,0} = [1 - c_4 (1 - \dot{n}_c)^2] (\dot{n}_c / \dot{G}_c) (2 - \dot{n}_c / \dot{G}_c) \quad (4)$$

where subscript 0 denotes design values, \dot{G}_c and \dot{n}_c are dimensionless flow rate and dimensionless rotating speed respectively, which can be calculated as follows,

$$\dot{G}_c = \frac{\dot{m}_c \sqrt{T_{c,in}} / P_{c,in}}{(\dot{m}_c \sqrt{T_{c,in}} / P_{c,in})_0} \quad (5)$$

$$\dot{n}_c = \frac{n_c \sqrt{T_{c,in}}}{(n_c \sqrt{T_{c,in}})_0} \quad (6)$$

and c_1 - c_4 are parameters, which can be calculated as follows,

$$\begin{cases} c_1 = \dot{n}_c / [q(1 - m / \dot{n}_c) + \dot{n}_c (\dot{n}_c - m)^2] \\ c_2 = (q - 2m\dot{n}_c^2) / [q(1 - m / \dot{n}_c) + \dot{n}_c (\dot{n}_c - m)^2] \\ c_3 = -(qm\dot{n}_c - m^2\dot{n}_c^3) / [q(1 - m / \dot{n}_c) + \dot{n}_c (\dot{n}_c - m)^2] \\ c_4 = 0.3 \end{cases} \quad (7)$$

As for the centrifugal compressors, $m = 1.8$ and $q = 1.8$. The efficiency of the compressor under off-design conditions can be optimized by changing the rotation speed, approaching its peak efficiency.

3.1.2 Turbine

The isentropic efficiency and power output of the turbine are shown as (8)-(9):

$$\eta_t = (h_{in,t} - h_{out,t}) / (h_{in,t} - h_{out,t,s}) \quad (8)$$

$$W_t = \dot{m}_t (h_{in,t} - h_{out,t}) \quad (9)$$

Off-design performance model of turbine is considered. Specifically, a modified Flügel formula is used [15,16], which is calculated as

$$\dot{G}_t = \sqrt{1.4 - 0.4\dot{n}_t} \sqrt{(1/\pi^2 - 1) / (1/\pi_0^2 - 1)} \quad (10)$$

$$\eta_t / \eta_{t,0} = [1 - 0.3(1 - \dot{n}_t)^2] (\dot{n}_t / \dot{G}_t) (2 - \dot{n}_t / \dot{G}_t) \quad (11)$$

$$\dot{G}_t = \frac{\dot{m}_t \sqrt{T_{t,in}} / P_{t,in}}{(\dot{m}_t \sqrt{T_{t,in}} / P_{t,in})_0} \quad (12)$$

$$\dot{n}_t = \frac{n_t \sqrt{T_{t,in}}}{(n_t \sqrt{T_{t,in}})_0} \quad (13)$$

3.1.3 Heat exchanger

The compression heat is stored separately in hot water to enhance the system efficiency. The heat released/absorbed by the sCO₂ is equal to the heat absorbed/released by the circulating water, satisfying the energy conservation equation,

$$\dot{m}_{sCO_2} (h_{sCO_2,in} - h_{sCO_2,out}) = \dot{m}_{water} (h_{water,out} - h_{water,in}) \quad (14)$$

3.1.4 Storage chamber

According to the conservation of energy and mass, the gas storage chamber can be described as

$$u\dot{m} + M \frac{du}{dt} = \dot{m}h \quad (15)$$

$$M = M_0 + \int_0^t \dot{m} dt \quad (16)$$

where \dot{m} represents the sCO_2 mass flow rate, which is positive during inflating and negative during deflating; u is the internal energy per unit mass of sCO_2 ; M is the sCO_2 mass in storage chamber; M_0 is the initial mass of sCO_2 in storage chamber; h is the enthalpy per unit mass of sCO_2 .

3.2 Performance criteria

In this paper, the round-trip efficiency ($\eta_{SC-CCES}$) and energy density ($E_{SC-CCES}$) are selected as system performance evaluation indicators.

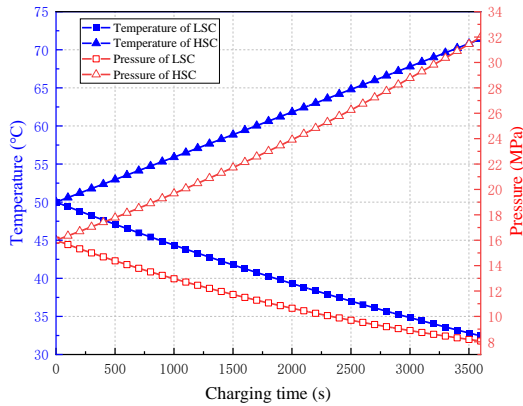
$$\eta_{SC-CCES} = \frac{\int_0^{t_{\text{discharge}}} W_t dt}{\int_0^{t_{\text{charge}}} W_c dt} \quad (17)$$

$$E_{SC-CCES} = \frac{\int_0^{t_{\text{discharge}}} W_t dt}{V_{\text{HSC}} + V_{\text{LSC}}} \quad (18)$$

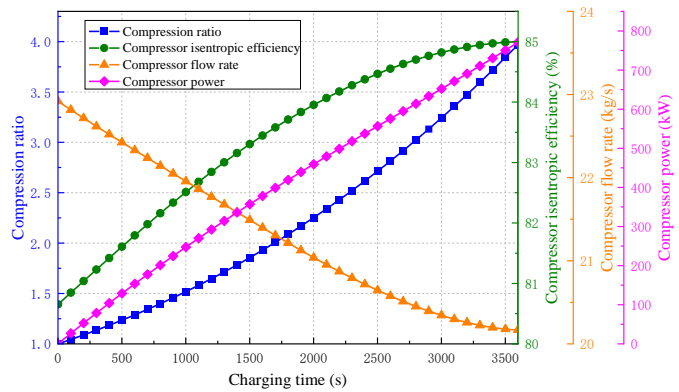
4. RESULTS AND DISCUSSION

4.1 System operation characteristics

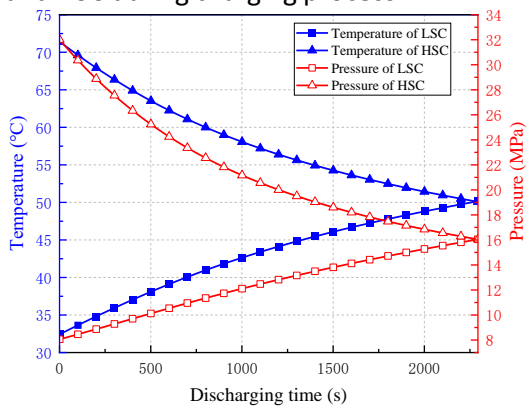
A typical case is selected to calculate the performance parameters of SC-CCES system to gain a preliminary assessment of system performance. The input parameters for a typical case [14,17] are listed in Table 1, and the design conditions for the compressor and turbine units are presented in Table 2. Fig. 2 (a) and (c) show the variation of temperature and pressure in HSC and LSC during charging and discharging process when the total charging time is 1 hour. The corresponding volume of HSC is 1000 m³ and LSC is 990 m³. During the operating process, continuous variation is observed in the temperature and pressure within the HSC and LSC, which results in the compressor and turbine unit unable to operate consistently at the design point. The operation characteristics of the compressor and turbine units under off-design conditions are illustrated in Fig. 2 (b) and (d). In Fig. 2 (b), the compression ratio consistently remains below ε_0 , except the terminal moment of charging process. However, even the compression ratio reaches ε_0 , the terminal temperature of charge in LSC is 32.4 °C, below $T_{c,0}$, ultimately



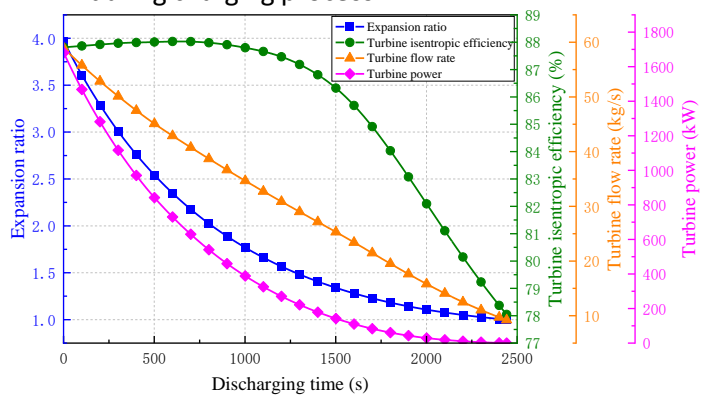
(a) Temperature and pressure variation in LSC and HSC during charging process



(b) Operation characteristics of compressor unit during charging process



(c) Temperature and pressure variation in LSC and HSC during discharging process



(d) Operation characteristics of turbine unit during discharging process

Fig. 2. System operation characteristics of the typical case

resulting in the compressor power remaining below 1 MW throughout the charging process. The round-trip efficiency of the typical system is 73.47 %, along with an energy density of 0.15 kWh/m³.

Table 1. Input parameters of the typical SC-CCES system

Parameters	Values
Initial pressure of charge in LSC and HSC, $P_{SC,init}$ (MPa)	16
Terminal pressure of charge in LSC, $P_{LSC,term}$ (MPa)	8
Terminal pressure of charge in HSC, $P_{HSC,term}$ (MPa)	32
Initial temperature of charge in LSC, $T_{LSC,init}$ (°C)	50
Initial temperature of charge in HSC, $T_{HSC,init}$ (°C)	50

Table 2. The design condition for the compressor and turbine units

Parameters	Values
Compressor isentropic efficiency, $\eta_{c,0}$ (%)	85
Compressor inlet pressure, $P_{c,0}$ (MPa)	8
Compressor inlet temperature, $T_{c,0}$ (°C)	35
Compression ratio, ε_0	4
Compressor flow rate, $\dot{m}_{c,0}$ (kg/s)	20
Compressor power, $W_{c,0}$ (MW)	1
Turbine isentropic efficiency, $\eta_{t,0}$ (%)	88
Turbine inlet pressure, $P_{t,0}$ (MPa)	28
Turbine inlet temperature, $T_{t,0}$ (°C)	60
Expansion ratio, π_0	2.6
Turbine flow rate, \dot{m}_t (kg/s)	50
Turbine power, $W_{t,0}$ (MW)	1

4.2 Parametric analysis

As the parametric analysis contributes to understanding the relationship between key input parameters and system performance, it is conducted to investigate the impact of seven critical parameters on the thermodynamics of SC-CCES system with round-trip efficiency and energy density as performance evaluation indicators. The key parameters considered in the SC-CCES system are initial pressure of charge in LSC and HSC ($P_{SC,init}$), terminal pressure of charge in LSC ($P_{LSC,term}$), terminal pressure of charge in HSC ($P_{HSC,term}$), initial temperature of charge in LSC ($T_{LSC,init}$), initial temperature of charge in HSC ($T_{HSC,init}$), compressor efficiency at design point ($\eta_{c,0}$) and turbine efficiency at

design point ($\eta_{t,0}$). When a specific parameter is studied for its effect on system performance, other parameters remain constant as Table 1 and Table 2 shown.

Fig. 3 (a) illustrates the effects of initial pressure of charge in LSC and HSC ($P_{SC,init}$) on SC-CCES system performance. As $P_{SC,init}$ decreases, the energy density and round-trip efficiency increase. Since the $P_{LSC,term}$ and $P_{HSC,term}$ of the SC-CCES remain constant (8 MPa and 32 MPa), the variation of pressure in HSC is increasing with $P_{SC,init}$ decreasing. Taking $P_{SC,init}$ equal 10 MPa as an example, the pressure in LSC decreases from 10 MPa to 8 MPa, while the pressure in HSC increases from 10 MPa to 32 MPa, during charging process. This leads to a significant increase in temperature within HSC, rising from 50 °C to 120 °C. Consequently, as the temperature of sCO₂ entering the turbine increases, it results in a rise in W_t , ultimately contributing to the enhancement of both round-trip efficiency and energy density.

Fig. 3 (b) displays the variation trend of the performance indicators of SC-CCES system under the variation of terminal pressure of charge in LSC ($P_{LSC,term}$). As $P_{LSC,term}$ increases, the pressure drop in LSC decreases during charging process, and pressure rise in LSC decreases during discharging process. This leads to an increase in volume of LSC, resulting energy density decreased. Furthermore, the compressor operates away from the design point due to the change of $P_{LSC,term}$, resulting in an increase in W_c during charging process and a decrease in round-trip efficiency. The factors contributing to the variations in Fig. 3 (c) are analogous to Fig. 3 (b). As $P_{HSC,term}$ decreases, the pressure rise in HSC decreases during charging process, and pressure drop in HSC decreases during discharging process, leading to an increase in volume of HSC and an increase in W_c .

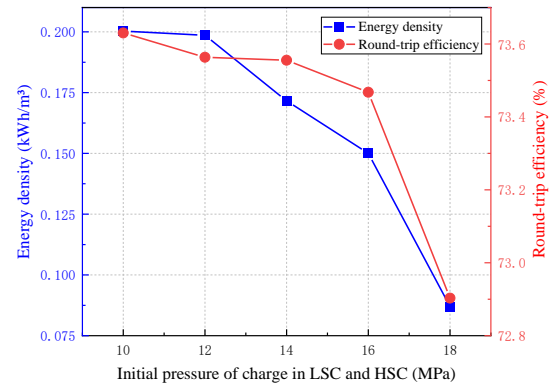
Fig. 3 (d) depicts the effects of the initial temperature of charge in LSC ($T_{LSC,init}$) on SC-CCES system performance. It highlights that the round-trip efficiency and energy density of SC-CCES system present opposite varying trends with $T_{LSC,init}$. As $T_{LSC,init}$ increases, the energy density increases, while the round-trip efficiency decreases. This is because the inlet temperature of compressor is equal to the temperature of the LSC, and the inlet temperature affects the efficiency of

compressor, leading to a reduction in round-trip efficiency. Besides, the outlet temperature of compressor and compression heat increase with compressor efficiency decreasing, which has impact on the inlet temperature of turbine. This leads to an increase in the power output of the turbine. Specifically, the power consumption increased by the compressor is greater than the counterpart increased by the turbine, which results in decreasing round-trip efficiency and increasing energy storage density.

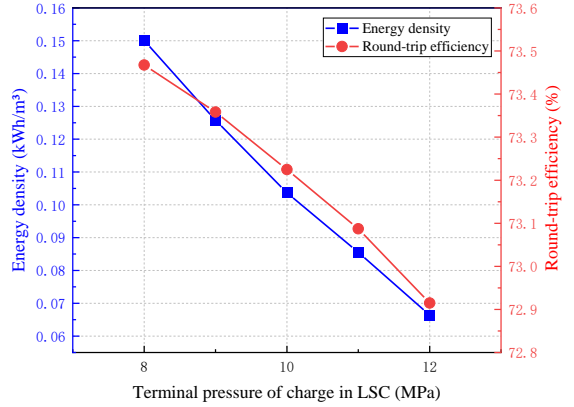
Fig. 3 (e) illustrates the effects of initial temperature of charge in HSC ($T_{HSC,init}$) on SC-CCES system performance. Due to the compressed sCO_2 being cooled to the same temperature as HSC, the temperature of sCO_2 entering HSC increases as $T_{HSC,init}$ increases. This leads to a reduction of the heat exergy degradation attributed to the heat transfer temperature difference in heat exchange process and an increase in the temperature of sCO_2 entering the turbine. As a result, both the energy density and round-trip efficiency are simultaneously enhanced.

Fig. 3 (f) shows the effects of compressor efficiency at design point ($\eta_{c,0}$) on SC-CCES system performance. The factors contributing to the variations in Fig. 3 (f) are analogous to Fig. 3 (d). On the one hand, as $\eta_{c,0}$ increases, the W_c decreases, resulting in round-trip efficiency increases. On the other hand, an increase in $\eta_{c,0}$ reduces the amount of compression heat, resulting in W_t decreases. Under this dual influence, the energy density increases as $\eta_{c,0}$ decreases. However, it should be noted that the rise of energy density is very slight, which implies that if other parameter conditions are altered, the trend may change.

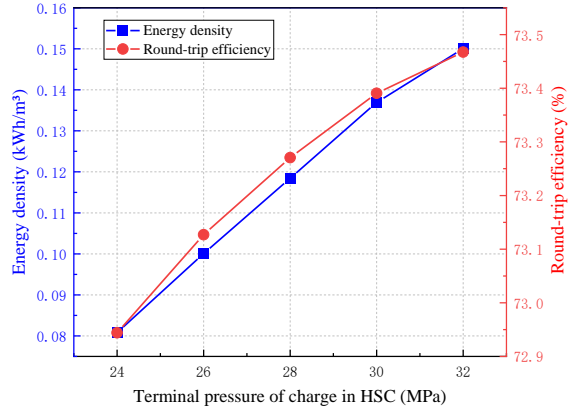
Fig. 3 (g) displays the effects of turbine efficiency at design point ($\eta_{t,0}$) on SC-CCES system performance. As $\eta_{t,0}$ increases, the W_t increases, consequently leading to a simultaneous enhancement in energy density and round-trip efficiency.



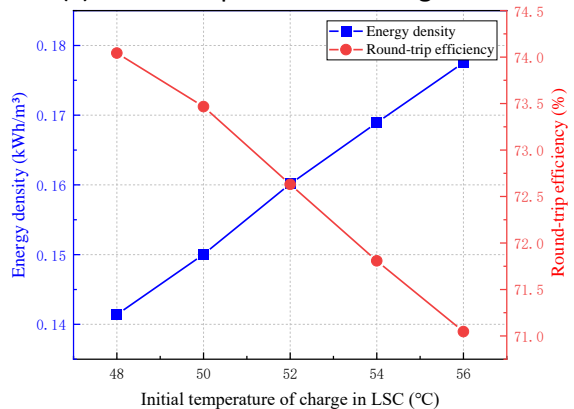
(a) Initial pressure of charge in LSC and HSC



(b) Terminal pressure of charge in LSC



(c) Terminal pressure of charge in HSC



(d) Initial temperature of charge in LSC

where $f(X)$ represents the objective function, w is weight factor, and p is normalization factor. According to Section 4.1, the performance parameters under typical operating conditions are employed as normalization factors, $p_1 = \frac{1}{\eta_{SC-CCES,typical}}$ and

$p_2 = \frac{1}{W_{SC-CCES,typical}}$. X represents variables, $g_i(X)$ and $h_j(X)$ are constraints. The last formula defines the search area, where X_k^L and X_k^U are the lower and upper bounds of the design variables, respectively.

The range of design variables are lists in Table 3 and the constraints are shown in Table 4. Table 5 displayed the AMGA properties. Fig. 4 shows the optimization process of SC-CCES system.

Table 3. Lower and upper boundaries of the design variables

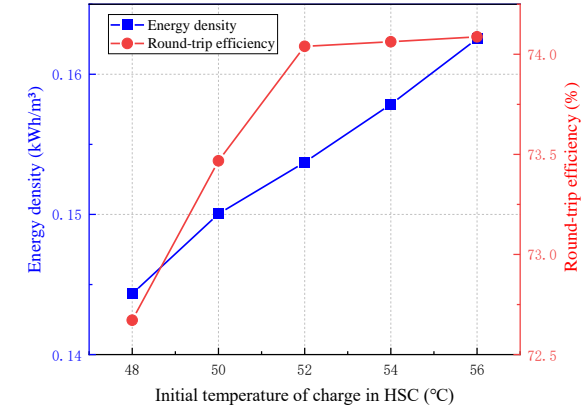
Parameters	Values
Initial pressure of charge in storage chamber, $P_{SC,init}$ (MPa)	8~32
Terminal pressure of charge in LSC, $P_{LSC,term}$ (MPa)	8~32
Terminal pressure of charge in HSC, $P_{HSC,term}$ (MPa)	8~32
Initial temperature of charge in LSC, $T_{LSC,init}$ (°C)	35~60
Initial temperature of charge in HSC, $T_{HSC,init}$ (°C)	35~60
Compressor efficiency at design point, $\eta_{c,0}$ (%)	70~90
Turbine efficiency at design point, $\eta_{t,0}$ (%)	70~90

Table 4. Constraints of SC-CCES system

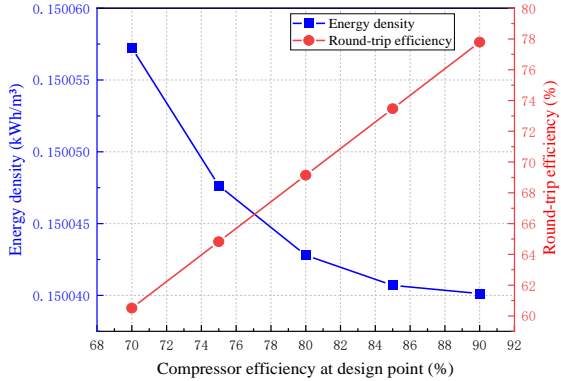
Parameters	Values
Temperature of LSC, T_{LSC} (°C)	> 31.3
Temperature of HSC, T_{HSC} (°C)	> 31.3
Initial-to-terminal pressure ratio of LSC, $P_{SC,init} / P_{LSC,term}$	> 1
Initial-to-terminal pressure ratio of HSC, $P_{SC,init} / P_{HSC,term}$	< 1
Mass ratio of hot water to cold water, $M_{water,hot} / M_{water,cold}$	> 1

Table 5. Properties of AMGA

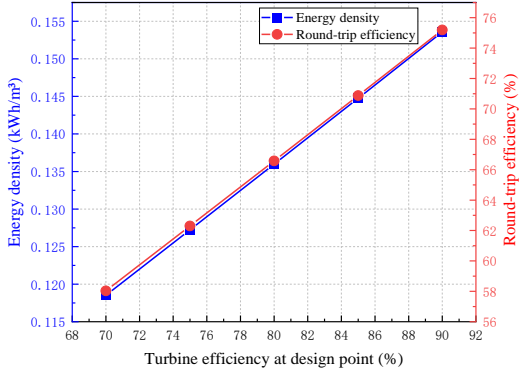
Parameters	Values
Initial size	40
Population size	40
Crossover probability	0.9
Mutation probability	0.5
Number of function evaluations	500



(e) Initial temperature of charge in HSC



(f) Compressor efficiency at design point



(g) Turbine efficiency at design point

Fig. 3. Effects of key input parameters on system performance

4.3 System optimization

The comprehensive performance of SC-CCES system could be improved by bi-objective optimization. In this paper, round-trip efficiency and energy density are selected as evaluation indicators for the system performance. Archive-based micro genetic algorithm (AMGA) is applied to optimize the comprehensive performance. The optimization model is as follows,

$$\begin{cases} \text{Max } f(X) = \text{Max } (w_1 p_1 \eta_{SC-CCES} + w_2 p_2 W_{SC-CCES}) \\ g_i(X) \leq 0 \\ h_j(X) = 0 \\ X_k^L \leq X_k \leq X_k^U \end{cases} \quad (19)$$

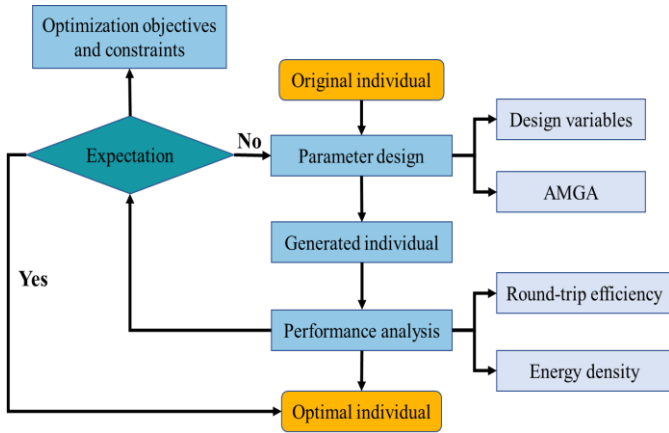


Fig. 4. Schematic of the optimization process

Table 6 and Fig. 5 presents the bi-objective optimization results of the SC-CCES system. The optimal round-trip efficiency is 78.14 %, along with the energy density is 0.2580 kWh/m³, when the two objectives are assigned equal weights.

Fig. 6 shows the effects of design variables on system performance in the objectives space. The optimal solution for the initial pressure of charge in LSC and HSC is around 12 MPa. Compared to round-trip efficiency, energy storage density is more responsive to fluctuations in the initial pressure of charge in LSC and HSC. The optimal solution for the terminal pressure of charge in LSC is 8 MPa, and the optimal solution for the terminal pressure of charge in HSC is 32 MPa, which are located at the boundaries of variables. It indicates that the potential for enhancing the overall performance of the system exists by expanding the operating ranges of compressor and turbine unit. The optimal solution for the initial temperature of charge in LSC is lower than the initial temperature of charge in HSC. With respect to the compressor, there is an optimal solution for isentropic efficiency, and the efficiency of turbine should be improved as much as possible.

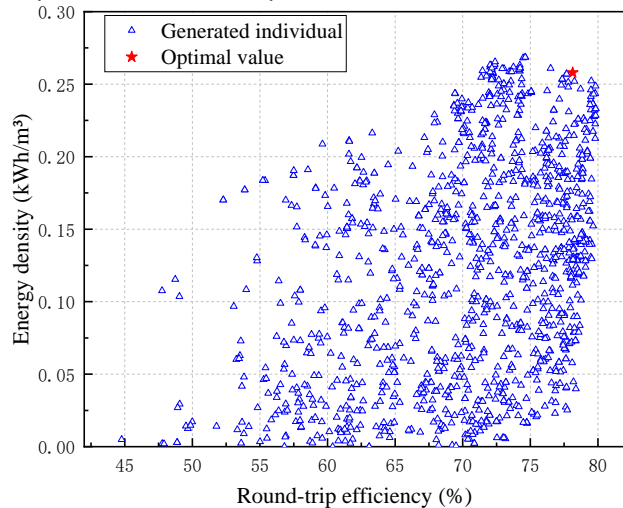
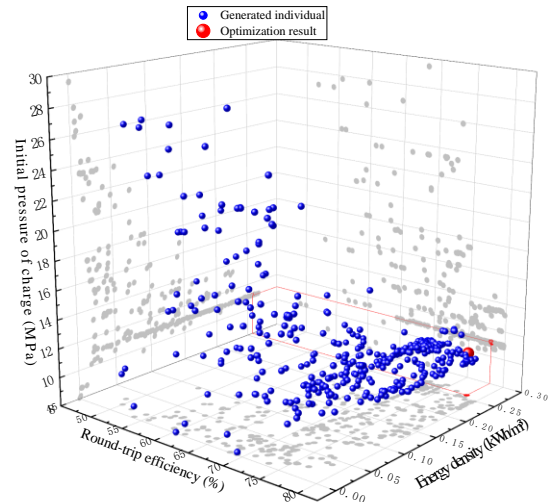


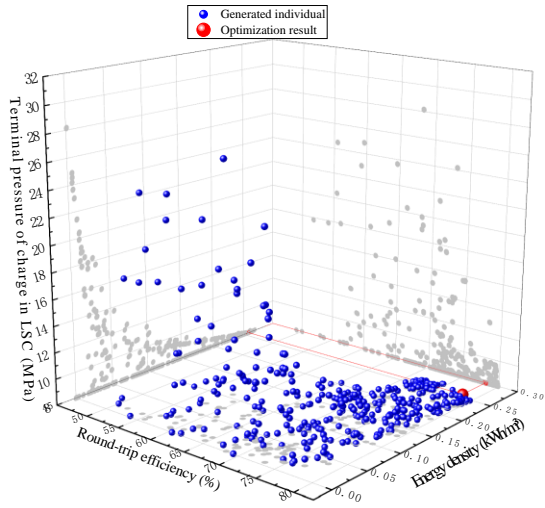
Fig. 5. System performance of optimization results

Table 6. Parameters of optimization results

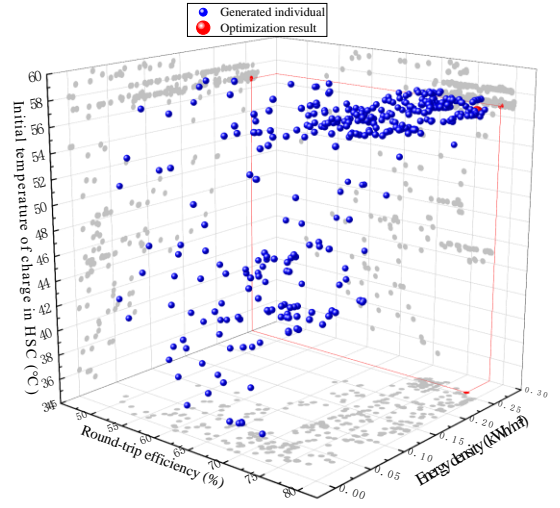
Parameters	Value
Weight factor of $\eta_{SC-CCES}, P_1$	0.5
Weight factor of $W_{SC-CCES}, P_2$	0.5
Initial pressure of charge in LSC and HSC, $P_{SC,init}$ (MPa)	11.09
Initial temperature of charge in LSC, $T_{LSC,init}$ (°C)	52.77
Initial temperature of charge in HSC, $T_{HSC,init}$ (°C)	56.79
Terminal pressure of charge in LSC, $P_{LSC,term}$ (MPa)	8.00
Terminal pressure of charge in HSC, $P_{HSC,term}$ (MPa)	32.00
Compressor isentropic efficiency $\eta_{c,0}$ (%)	0.87
Turbine isentropic efficiency $\eta_{t,0}$ (%)	0.90
Round-trip efficiency, $\eta_{SC-CCES}$ (%)	78.14
Energy storage density, $W_{SC-CCES}$ (kWh/m ³)	0.2580



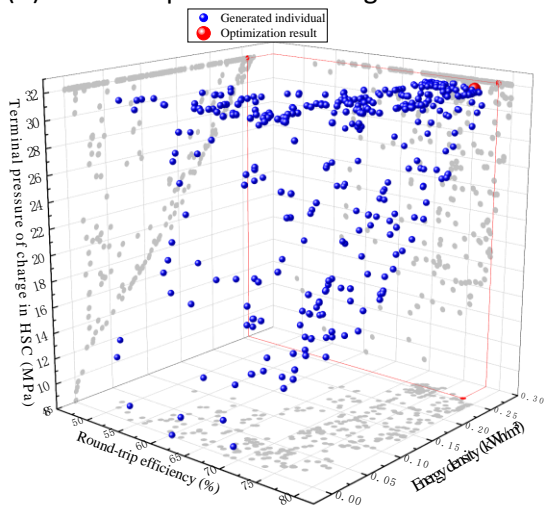
(a) Initial pressure of charge in LSC and HSC



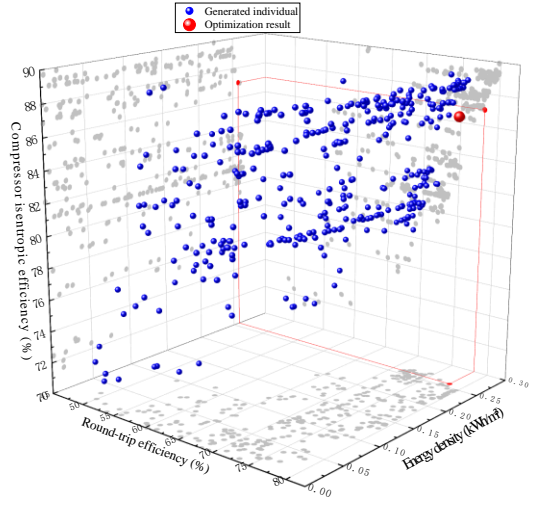
(b) Terminal pressure of charge in LSC



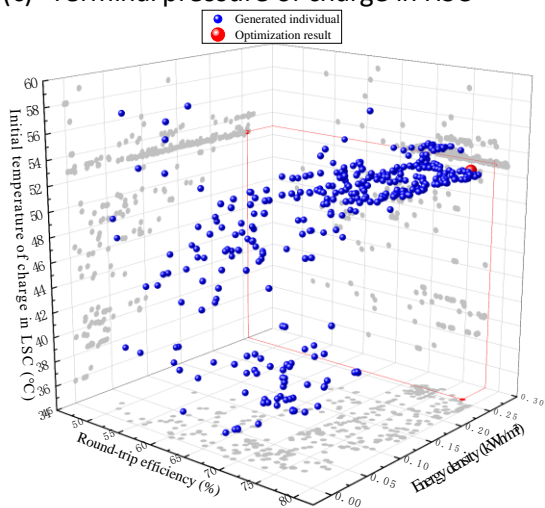
(e) Initial temperature of charge in HSC



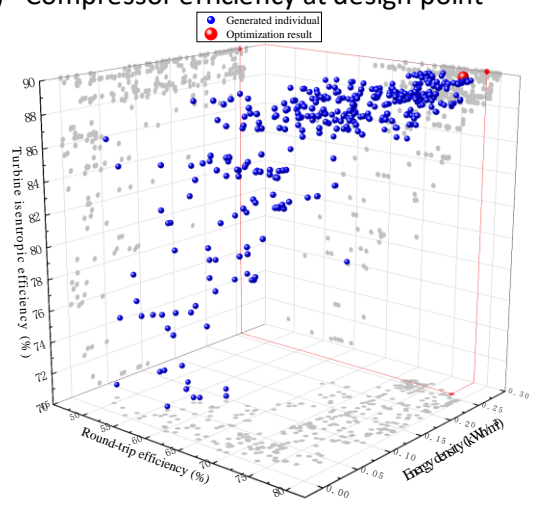
(c) Terminal pressure of charge in HSC



(f) Compressor efficiency at design point



(d) Initial temperature of charge in LSC



(g) Turbine efficiency at design point

Fig. 6. Effects of design variables on system performance in the objectives space

5. CONCLUSIONS

In order to reveal the thermal characteristics of a supercritical compressed CO₂ energy storage (SC-CCES)

system under actual working conditions, this paper carries out off-design performance analysis and optimization of the system. The main conclusions are summarized as follows:

(1) In the process of charging and discharging of the SC-CCES system, the pressure and temperature of the low-pressure and high-pressure storage chamber continue to change, resulting in the compressor and turbine continue to operate under off-design conditions. In the process of charging, the compression ratio increases from 1 to 4, and the minimum compressor efficiency deviation from the design point of 5.11%. In the process of discharging, the expansion ratio decreases from 4 to 1, and the minimum turbine efficiency deviation from the design point of 11.31%.

(2) The results of parametric analysis indicate that the efficiencies of compressor and turbine have the greatest impact on system performance. Furthermore, the round-trip efficiency and energy density of SC-CCES system present opposite varying trends with increasing compressor efficiency and initial temperature of charge in low-pressure storage chamber.

(3) Round-trip efficiency and energy density cannot reach the optimum values simultaneously. The optimal round-trip efficiency of SC-CCES system is achieved as 78.14 %, along with the optimal energy density of 0.2580 kWh/m³.

ACKNOWLEDGEMENT

The authors acknowledge support from the Natural Science Foundation of China (2022YFB2405201) and the National Youthful Science Foundation of China (No. 52206031).

DECLARATION OF INTEREST STATEMENT

The authors declare that they have no known competing financial interests or personal relationships that could have appeared to influence the work reported in this paper. All authors read and approved the final manuscript.

REFERENCE

[1] Gangopadhyay A, Seshadri A K, Patil B. Wind-solar-storage trade-offs in a decarbonizing electricity system. *Appl Energy* 2024; 353: 121994.
[2] He Z, Liu C, Wang Y, et al. Optimal operation of wind-solar-thermal collaborative power system considering carbon trading and energy storage. *Appl Energy* 2023; 352: 121993.
[3] Sun W, Liu X, Yang X, et al. Design and thermodynamic performance analysis of a new liquid carbon dioxide

energy storage system with low pressure stores. *Energ Convers Manage* 2021; 239: 114227.

[4] Chae Y J, Lee J I. Thermodynamic analysis of compressed and liquid carbon dioxide energy storage system integrated with steam cycle for flexible operation of thermal power plant. *Energ Convers Manage* 2022; 256: 115374.

[5] Xu M, Zhao P, Huo Y, et al. Thermodynamic analysis of a novel liquid carbon dioxide energy storage system and comparison to a liquid air energy storage system. *J Clean Prod* 2020; 242: 118437.

[6] Liu X, Yan X, Liu X, et al. Comprehensive evaluation of a novel liquid carbon dioxide energy storage system with cold recuperator: Energy, conventional exergy and advanced exergy analysis. *Energ Convers Manage* 2021; 250: 114909.

[7] Li Y, Yu H, Tang D, et al. A comparison of compressed carbon dioxide energy storage and compressed air energy storage in aquifers using numerical methods. *Renew Energ* 2022; 187: 1130-1153.

[8] Xu W, Zhao P, Gou F, et al. A combined heating and power system based on compressed carbon dioxide energy storage with carbon capture: Exploring the technical potential. *Energ Convers Manage* 2022; 260: 115610.

[9] Liu H, He Q, Borgia A, et al. Thermodynamic analysis of a compressed carbon dioxide energy storage system using two saline aquifers at different depths as storage reservoirs. *Energ Convers Manage* 2016; 127: 149-159.

[10] Wu C, Wan Y, Liu Y, et al. Thermodynamic simulation and economic analysis of a novel liquid carbon dioxide energy storage system. *J Energy Storage* 2022, 55: 105544.

[11] Li H, Ju Y, Zhang C. Optimization of supercritical carbon dioxide recompression Brayton cycle considering anti-condensation design of centrifugal compressor. *Energ Convers Manage* 2022; 254: 115207.

[12] Saeed M, Khatoon S, Kim M H. Design optimization and performance analysis of a supercritical carbon dioxide recompression Brayton cycle based on the detailed models of the cycle components. *Energ Convers Manage* 2019; 196: 242-260.

[13] Xu M, Wang X, Wang Z, et al. Preliminary design and performance assessment of compressed supercritical carbon dioxide energy storage system. *Appl Therm Eng* 2021; 183: 116153.

[14] He Q, Liu H, Hao Y, et al. Thermodynamic analysis of a novel supercritical compressed carbon dioxide energy storage system through advanced exergy analysis. *Renew Energ* 2018; 127: 835-849.

- [15] Zhang N, Cai R. Analytical solutions and typical characteristics of part-load performances of single shaft gas turbine and its cogeneration. *Energ Convers Manage* 2002; 43(9-12): 1323-1337.
- [16] Zhang H, Wang L, Lin X, et al. Combined cooling, heating, and power generation performance of pumped thermal electricity storage system based on Brayton cycle. *Appl Energy* 2020; 278: 115607.
- [17] Zhang X R, Wang G B. Thermodynamic analysis of a novel energy storage system based on compressed CO₂ fluid. *Int J Energ Res* 2017; 41(10): 1487-1503.